1366 *Chem. Mater.* **1998,** *10,* 1366−1373

Variations on a One-Dimensional Theme: The Hydrothermal Syntheses of Inorganic/Organic Composite Solids of the Iron Molybdate Family

Pamela J. Zapf,[†] Robert P. Hammond,[†,‡] Robert C. Haushalter,[§] and
Jon Zubieta*,[†]

Department of Chemistry, Syracuse University, Syracuse, New York 13244,
NEC Research Institute, 4 Independence Way, Princeton, New Jersey 08540, and
Symyx Technologies, 3100 Central Expressway, Santa Clara, California 95051

Received November 20, 1997. Revised Manuscript Received March 5, 1998

The hydrothermal reactions of molybdenum oxide starting materials with iron(II) and iron(III) halides in the presence of 2,2′-bipyridine have afforded the three related one-dimensional solid materials $[MoO_4\{Fe(III)Cl(2,2'\text{-}bpy)\}]$ (**1**), $[Mo_3O_{12}\{Fe(III)(2,2'\text{-}bpy)\}_2]\cdot 0.25H_2O$ (**2**), and $[Mo_4O_{15}\{Fe(III)(2,2'\text{-}bpy)\}_2]$ (**3**). The structures of these three materials are based on a common one-dimensional ribbon exhibited by **1**. The ribbon is constructed from four-polyhedra rings consisting of two $\{MoO_4\}$ tetrahedra and two $\{FeXN_2O_3\}$ (X = Cl for **1**, O for **2** and **3**) octahedra. These polyhedra corner share such that each molybdenum center serves to bridge the two iron octahedra in the ring. Attachment to the next such four-ring is through the third corner sharing interaction of each molybdenum tetrahedron. Replacement of the pendant chloride substituents on adjacent iron centers in **1** with an $\{MoO_4\}$ unit leads to compound **2**, while an $\{Mo_2O_7\}$ linkage between adjacent iron centers affords **3**.

Introduction

Metal oxide based solid phases have received considerable attention due to their applications in catalysis, sorption, energy storage, molecular electronics, optical materials, and ceramics.[1,2] Exploitation of hydrothermal techniques in combination with introduction of organic components that possess structure-directing properties has allowed the isolation of metastable inorganic/organic composites which retain some structural features of their synthetic precursors.[3] Typically, the organic substituents have been present as charge-compensating cations such as organoammonium units. Examples of such compounds include the one-dimensional $[H_3NCH_2CH_2NH_3][Mo_3O_{10}]$[4] and $[H_3N(CH_2)NH_3][Mo_4O_{13}]$[5] and the two-dimensional phases $[4,4'\text{-}H_2bpy][Mo_7O_{22}]\cdot H_2O$,[6] $[H_3N(CH_2)_3NH_3][V_4O_{10}]$,[7] and $[HN(C_2H_4)_3NH][V_6O_{14}]\cdot H_2O$.[8]

In other recent applications, the organic substituents have been introduced as ligands covalently linked to the inorganic backbone of the solid. Such materials include the one-dimensional vanadium oxide phases $[VO(VO_3)_6\{VO(2,2'\text{-}bpy)_2\}_2]$[9] and $[V^{IV}V^{V}_2O_7(phen)]_n$[10] and the three related one-dimensional molybdenum oxide phases $[MoO_3(2,2'\text{-}bpy)]$, $[Mo_2O_6(2,2'\text{-}bpy)]$, and $[Mo_3O_9(2,2'\text{-}bpy)_2]$.[11] Another mode of attachment observed for these ligands is as "tethers" between metal sites, a modality commonly adopted by 4,4′-bipyridine as seen in $[MoO_3(4,4'\text{-}bpy)_{0.5}]$,[12] for example. Incorporation of complex transition metal/organic components into the covalent backbone of metal oxide solids, either as peripheral moieties or as complex bridging units, has also been reported, including such vanadium oxide based examples as $[(2,2'\text{-}bpy)Zn]_2[V_6O_{17}]$[13] and the three related phases $[Cu(H_2N(CH_2)_2NH_2)][V_2O_6]$, $[Cu(2,2'\text{-}bpy)][V_2O_6]$, and $[Cu(2,2'\text{-}bpy)_2][V_2O_6]$.[14] Examples based on molybdenum oxides include the one-dimensional $[Ni(2,2'\text{-}bpy)_2Mo_4O_{13}]$ and $[Cu(2,2'\text{-}bpy)Mo_2O_7]$ and the two-dimensional $[Co(2,2'\text{-}bpy)Mo_3O_{10}]$[15] and $[\{Ni(H_2O)_2(4,4'\text{-}bpy)_2\}_2Mo_8O_{26}]$.[16]

In terms of the metal oxide compositions, these latter hybrid materials are related to the mixed metal molybdates, $[M_x(MoO_4)_y]$, of which the phases $[FeMoO_4]$[17]

[†] Syracuse University.
[‡] NEC Research Institute.
[§] Symyx Technologies.

(1) Cheetham, A. K. *Science* **1994**, *264*, 794 and references therein.
(2) Cox, P. A. *Transition Metal Oxides*; Clarendon Press: Oxford, England, 1995.
(3) Gopalakrishnan, J. *Chem. Mater.* **1995**, *7*, 1265.
(4) Khan, M. I.; Chen, Q.; Zubieta, J. *Inorg. Chim. Acta* **1993**, *213*, 328.
(5) Xu, Y.; An, L.-H.; Koh, L.-L. *Chem. Mater.* **1996**, *8*, 814.
(6) Zapf, P. J.; Haushalter, R. C.; Zubieta, J. *Chem. Commun.* **1997**, 321.
(7) Zhang, Y.; O'Connor, C. J.; Clearfield, A.; Haushalter, R. C. *Chem. Mater.* **1996**, *8*, 595.
(8) Zhang, Y.; Haushalter, R. C.; Clearfield, A. *Chem. Commun.* **1996**, 1055.
(9) Huan, G.; Johnson, J. W.; Jacobson, A. J.; Merola, J. S. *J. Solid State Chem.* **1991**, *91*, 385.
(10) Duan, C.-y.; Tian, Y.-p.; Lu, Z.-l.; You, X.-z. *Inorg. Chem.* **1995**, *34*, 1.
(11) Zapf, P. J.; Haushalter, R. C.; Zubieta, J. *Chem. Mater.* **1997**, *9*, 2019.
(12) (a) Johnson, J. W.; Jacobson, A. J.; Rich, S. M.; Brody, J. F. *J. Am. Chem. Soc.* **1981**, *103*, 5346. (b) Zapf, P. J.; LaDuca, R. L.; Warren, C. J.; Zubieta, J., unpublished results.
(13) Zhang, Y.; DeBord, J. R. D.; O'Connor, C. J.; Haushalter, R. C.; Clearfield, A.; Zubieta, J. *Angew. Chem., Int. Ed. Engl.* **1996**, *35*, 989.
(14) DeBord, J. R. D.; Zhang, Y.; Haushalter, R. C.; Zubieta, J.; O'Connor, C. J. *J. Solid State Chem.*, **1996**, *122*, 251.

and $[Fe_2(MoO_4)_3]$[18] are of particular relevance to the work presented herein. At least three polymorphs of $[FeMoO_4]$ have been reported, including a low-temperature, low-pressure modification, α-$[FeMoO_4]$; a high-temperature, low-pressure form, β-$[FeMoO_4]$; and a high-pressure modification, $[FeMoO_4]$-II.[17] The structure of α-$[FeMoO_4]$ was reported to be isotypic with α-$[CoMoO_4]$[19] by Sleight et al., while the structure of β-$[FeMoO_4]$ was reported to be isotypic with that of α-$[MnMoO_4]$.[20] In both α-$[CoMoO_4]$ and α-$[MnMoO_4]$, there are two crystallographically independent Mo atoms and two crystallographically independent M atoms (where M = Mn, Co). The arrangement of oxygen atoms about the Mn and Co atoms in both α-$[CoMoO_4]$ and α-$[MnMoO_4]$ generates distorted octahedra. However, the Mo coordination sites in α-$[CoMoO_4]$ are distorted octahedra while in α-$[MnMoO_4]$ the Mo centers are surrounded by slightly distorted oxygen tetrahedra. The structure of $[Fe_2(MoO_4)_3]$ consists of four crystallographically distinct $\{FeO_6\}$ octahedra and six unique $\{MoO_4\}$ tetrahedra sharing corners such that each iron octahedron is linked to six molybdenum tetrahedra while each tetrahedra is linked to four octahedra. Thus, every oxygen in $[Fe_2(MoO_4)_3]$ is linked to an iron and a molybdenum.

While the fundamental structural units of the compounds presented in this study bear a superficial resemblance to those seen in such dense phase iron molybdates, the effects of introducing organic substituents are manifest in significant differences in the extended structures. "Passivation" of the iron centers through use of 2,2′-bipyridine, which occupies sites on the metal coordination sphere, has precluded the formation of dense phases or even two-dimensional iron molybdates by blocking further Fe−oxo bond formation. This "passivation" of the iron centers has allowed the isolation of a series of one-dimensional inorganic/organic composite materials $[MoO_4\{Fe(III)Cl(2,2'\text{-}bpy)\}]$ (**1**), $[Mo_3O_{12}\{Fe(III)(2,2'\text{-}bpy)\}_2]\cdot 0.25\ H_2O$ (**2**), and $[Mo_4O_{15}\{Fe(III)(2,2'\text{-}bpy)\}_2]$ (**3**).

Experimental Section

Reagents were purchased from Aldrich Chemical Co. and used without further purification. All syntheses were carried out in 23 mL poly(tetrafluoroethylene)-lined stainless steel containers under autogenous pressure. The reactants were stirred briefly before heating. All distilled water used was distilled above 3.0 Ω in-house using a Barnstead Model 525 Biopure Distilled Water Center.

Synthesis of $[MoO_4\{FeCl(2,2'\text{-}bpy)\}]$ (1). A mixture of $Na_2MoO_4\cdot 2H_2O$ (0.0548 g), MoO_3 (0.0312 g), 2,2′-bipyridine (0.0711 g), $FeCl_2\cdot 4H_2O$ (0.1763 g), and H_2O (8.048 g) in the mole ratio 1:0.96:2.01:3.92:1970 was heated at 160 °C for 164 h. After cooling for 3 h, the solid products were collected by filtration. A yellow plate of **1** suitable for single-crystal X-ray diffraction was selected from a mixture of yellow plates, fine colorless needles, and a small amount of red powder. The initial pH of the reaction mixture after brief stirring was 5.3, while the final pH was found to be 1.0. Yield of **1** was ca. 5%. Anal. Calcd For $C_{10}H_8N_2O_4ClFeMo$: C, 29.5; H, 1.98; N, 6.88. Found: C, 29.2; H, 1.87; N, 7.01. μ_{eff} at 293 K: 5.94 μ_B.

Synthesis of $[Mo_3O_{12}\{Fe(2,2'\text{-}bpy)\}_2]\cdot 0.25\ H_2O$ (2). Compound **2** was synthesized from a reaction mixture of $Na_2MoO_4\cdot 2H_2O$ (0.1607 g), 2,2′-bipyridine (0.1034 g), $FeBr_2\cdot$(0.1420 g), and H_2O (6.037 g) in the mole ratio 1:1:0.99:503 and heated to 160 °C for 88 h. After cooling for 3 h, the solid products were collected by filtration, and large yellow plates of **2** were mechanically separated from a mixture of **2**, colorless rods, and unidentified tan and red powders. The colorless rods were identified as $MoO_3(2,2'\text{-}bpy)$ by X-ray diffraction.[11] The initial pH of the reaction mixture after brief stirring was 6.0, while the final pH was found to be 6.1. Yield of **2** is ca. 20%. Anal. Calcd for $C_{20}H_{16.5}N_4O_{12.25}Fe_2Mo_3$: C, 26.4; H, 1.83; N, 6.17. Found: C, 26.6; H, 1.70; N, 6.25. μ_{eff} at 293 K: 5.92 μ_B.

Synthesis of $[Mo_4O_{15}\{Fe(2,2'\text{-}bpy)\}_2]$ (3). A mixture of $Na_2MoO_4\cdot 2H_2O$ (0.1067 g), 2,2′-bipyridine (0.0699 g), $FeCl_3\cdot 6H_2O$ (0.1197 g) and H_2O (8.019 g), in the mole ratio 1:1:1:1010 was heated to 200 °C. After cooling under ambient conditions for 3 h, the solid products were filtered, yielding yellow plates of **3**, green square plates, and a small amount of red powder. The yellow-green plates were later identified as $Fe_2(MoO_4)_3$ by single-crystal X-ray diffraction.[21] Although yellow crystals of **3** were observed as a product of this reaction for reaction times between 24 and 168 h, optimal yield of solid product (69%) was obtained at 144 h. However, optimal crystal quality for single-crystal X-ray diffraction studies (as ascertained by visual inspection of the products) was obtained at 48 h. The initial pH of the reaction mixture after brief stirring was 2.2, while the final pH was found to be 1.1. Anal. Calcd For $C_{20}H_{16}N_4O_{15}Fe_2Mo_4$: C, 22.9; H, 1.54; N, 5.35. Found: C, 22.5; H, 1.42; N, 5.22. μ_{eff} at 293 K: 5.95 μ_B.

X-ray Crystallography. Structural measurements for compounds **1**−**3** were performed on a Siemens SMART-CCD diffractometer using graphite monochromated Mo Kα radiation (λ(Mo Kα) = 0.71073 Å).

The data for **1**−**3** were collected at a temperature of 150 ± 1 K and were corrected for Lorentz and polarization effects. The structures of **2** and **3** were solved by direct methods[22] while that of **1** was solved utilizing the Patterson method. All non-hydrogen atoms in **1**−**3** were refined anisotropically. Neutral atom scattering coefficients and anomalous dispersion corrections were taken from the International Tables, volume C.[23] All calculations were performed using the SHELXTL[24] crystallographic software package except as described for **1**, below.

Crystals of compound **1** exhibited nonmerohedral twinning which required the use of a set of programs supplied by Bruker Analytical X-ray Systems, Inc. (formerly Siemens Analytical Instruments, Inc.). Using the program SAINT[25] with each of two contributing orientation matrixes and the frames of raw data collected by SMART,[26] two sets of integrated intensities were generated. Using the program TWHKL,[27] each reflection from the two sets was placed into one of three categories: (1) reflections from the two twin components with almost exact overlap, (2) reflections from the two twin components with partial overlap, and (3) reflections from the two twin components which do not overlap. Two sets of indices (one from each

---

(15) Zapf, P. J.; Warren, C. J.; Haushalter, R. C.; Zubieta, J. *Chem. Commun.* **1997**, 1543.

(16) Hagrman, D.; Zubieta, C.; Rose, D. J.; Zubieta, J.; Haushalter, R. C. *Angew. Chem., Int. Ed. Engl.* **1997**, *36*, 873.

(17) Sleight, A. W.; Chamberland, B. L.; Weiher, J. F. *Inorg. Chem.* **1968**, *7*, 1093 and references therein.

(18) (a) Rapposch, M. H.; Anderson, J. B.; Kostiner, E. *Inorg. Chem.* **1980**, *19*, 3531. (b) Plyasova, L. M.; Klevtsova, R. F.; Borisov, S. V.; Kefeli, L. M. *Sov. Phys.-Dokl. (Engl. Transl.)* **1966**, *11*, 189.

(19) Smith, G. W.; Ibers, J. A. *Acta Crystallogr.* **1965**, *19*, 269.

(20) Abrahams, S. C.; Reddy, J. M. *J. Chem. Phys.* **1965**, *43*, 2533.

(21) Rapposch, M. H.; Anderson, J. B.; Kostiner, E. *Inorg. Chem.* **1980**, *19*, 3531 and references therein.

(22) SHELXTL PC Siemens Analytical X-ray Instruments, Inc., Madison, WI, 1993.

(23) International Tables for Crystallography, Volume C, Tables 4.2.6.8 and 6.1.1.4.

(24) Sheldrick, G. M. SHELXTL PC. Version 5.0. Siemens Analytical Instruments Inc., Madison, WI, 1994.

(25) SAINT Data Reduction Software. Version 4.050. Siemens Analytical Instruments Inc., Madison, WI, 1996.

(26) SMART. Data Collection Software. Version 4.050. Siemens Analytical Instruments Inc., Madison, WI, 1996.

(27) Sparks, R. A. TWINDX, TWUTIL, TWHKL, TWROT. Nonmerohedral Twinning Software. Beta test version. Bruker Analytical X-ray Systems, Inc., Madison, WI, 1997.

Table 1. Crystallographic Data for the One-Dimensional Solids [MoO_4{FeCl(2,2′-bpy)}] (1), [Mo_3O_{12}{Fe(2,2′-bpy)}$_2$]·0.25 H_2O (2), and [Mo_4O_{15}{Fe(2,2′-bpy)}$_2$] (3)

	1	2	3
chemical formula	$C_{10}H_8ClFeMoN_2O_4$	$C_{20}H_{16.5}Fe_2Mo_3N_4O_{12.25}$	$C_{20}H_{16}Fe_2Mo_4N_4O_{15}$
a, Å	6.8578(4)	10.7592(3)	10.9239(2)
b, Å	17.6131(9)	11.1192(3)	11.0210(3)
c, Å	10.3890(5)	12.6225(3)	13.5564(3)
α, deg	90	75.091(1)	88.30
β, deg	102.562(1)	71.181(1)	88.497(1)
γ, deg	90	69.131(1)	65.293(1)
V, Å^3	1224.82(11)	1318.17(6)	1481.86(6)
Z	4	2	2
fw	407.42	908.39	1047.83
space group	$P2_1/c$	P-1	P-1
T, K	150	150	150
λ, Å	0.71073	0.71073	0.71073
D_{calc}, g cm^{-3}	2.209	2.289	2.348
μ, mm^{-1}	2.435	2.533	2.670
R^a	0.0435	0.0663	0.0456
$wR2^b$	0.1069	0.1592	0.0919
data/parameters	7355/173	5826/374	6450/406

[a] $\Sigma||F_o| - |F_c||/|F_o|$. [b] $[\Sigma[w(F_o^2 - F_c^2)^2]/\Sigma[w(F_o^2)^2]]^{1/2}$.

component) were assigned to those reflections in the first category. One set of indices was assigned to those reflections in the third category. The reflections in the second category were discarded. TWHKL generated a file containing reflection indices and squared structure factors from the first and third categories. This file was then used as input to SHELXTL which did a least-squares refinement of the atomic parameters. This program also refined the volume fraction of one of the twin components. Finally, the program TWROT[27] determined the rotation axis for the twinning operation from the two orientation matrixes. It was determined that the orientation of the second twin component is related to the first by a rotation of 180° about the normal to the 0 0 1 face of the crystal. After the use of Sparks' Non-merohedral Twinning Software, refinement of the solution for **1** was unexceptional.

Crystallographic data for **1**−**3** are listed in Table 1. Atomic positional parameters and isotropic temperature factors for **1**−**3** are given in Table 2. Selected bond lengths and angles for **1**−**3** are listed in Table 3.

Results and Discussion

Hydrothermal synthesis and other soft-chemical techniques have previously proved useful for the isolation of a wide variety of metastable oxide phases.[3,28] Exploitation of the hydrothermal method has allowed the isolation of a related series of one-dimensional organic/inorganic composite materials reported in this study: [MoO_4{FeCl(2,2′-bpy)}] (**1**), [Mo_3O_{12}{Fe(2,2′-bpy)}$_2$]·0.25 H_2O (**2**), and [Mo_4O_{15}{Fe(2,2′-bpy)}$_2$] (**3**). Hydrothermal syntheses of **1**−**3** were carried out in Teflon-lined stainless steel Parr acid digestion bombs at temperatures of either 160 or 200 °C and autogenous pressures. It is interesting to note that although the oxidation state of the iron in compounds **1**, **2**, and **3** is +3, the starting materials for **1** and **2** contained Fe(II). Attempts to reproduce the syntheses of **1** and **2** using Fe(III) starting materials have, thus far, proved unsuccessful.

The hydrothermal reaction of a mixture of Na_2MoO_4·2H_2O, MoO_3, 2,2′-bipyridine, $FeCl_2$·4H_2O, and H_2O for 164 h at 160 °C yields the one-dimensional material [MoO_4{FeCl(2,2′-bpy)}] (**1**). Likewise, reaction of a mixture of Na_2MoO_4·2H_2O, 2,2′-bipyridine, $FeBr_2$, and H_2O at 160 °C for 88 h gives [Mo_3O_{12}{Fe(2,2′-bpy)}$_2$]·0.25 H_2O (**2**). Compound **3**, [Mo_4O_{15}{Fe(2,2′-bpy)}$_2$], is synthesized in good yield by reacting a mixture of Na_2MoO_4·2H_2O, 2,2′-bipyridine, $FeCl_3$·6H_2O, and H_2O at 200 °C for 24 to 168 h. As often observed in hydrothermal syntheses, there is no apparent correlation between the composition of the product and reaction stoichiometries employed. However, it is clear that the identity of the product obtained in hydrothermal reactions is critically dependent on the specific reaction conditions employed, as evidenced by the lack of success in synthesizing compounds **1** and **2** using Fe(III) starting materials.

As shown in Figure 1a, the structure of [MoO_4{FeCl(2,2′-bpy)}] (**1**) consists of one-dimensional chains comprised of {$FeClN_2O_3$} octahedra and {MoO_4} tetrahedra. Every iron octahedron corner shares through each of its oxygens with an adjacent {MoO_4} unit while each {MoO_4} unit serves to bridge three iron octahedra. The terminal chlorides on the iron sites alternate such that two adjacent {$FeClN_2O_3$} octahedra will have their chloride substituents oriented to opposite sides of the chain as shown in Figure 2a.

The structure of [Mo_3O_{12}{Fe(2,2′-bpy)}$_2$]·0.25 H_2O (**2**), shown in Figure 1b, consists of chains constructed from {FeN_2O_4} octahedra and {MoO_4} tetrahedra. In the case of compound **1**, all adjacent iron octahedra are linked through two {$MoO_{3/2}O$} tetrahedra. In contrast, in **2** there are additional corner sharing interactions between pairs of adjacent {FeN_2O_4} octahedra and an additional {$MoO_{2/2}O_2$} tetrahedron, as illustrated in Figure 1b. Consequently, adjacent pairs of {FeN_2O_4} octahedra are linked through three {MoO_4} tetrahedra. These units comprised of two iron centers and three molybdenum centers are then linked to a neighboring {Fe_2Mo_3} unit via two corner sharing interactions. Thus, the connectivity of adjacent iron sites in the chain alternates between linkage through three {MoO_4} tetrahedra and linkage through two {MoO_4} tetrahedra. The orientations of the additional {$MoO_{2/2}O_2$} units in **2** with respect to the chain structure of **1** alternate so as to occupy opposite sides of the chain, shown in Figure 2b. It should be noted that this apparent substitution of an {$MoO_{2/2}O_2$} unit for adjacent chlorides requires a reorientation of the iron polyhedron as the chloride sites are located on opposite sides of the chain in **1**.

---

(28) Stein, A.; Keller, S.; Mallouk, T. E. *Science* **1993**, *259*, 1558.

Table 2. Atomic Positional Parameters [×10^4] and Equivalent Isotropic Displacement Parameters [$Å^2 \times 10^3$] for the One-Dimensional Solids [MoO_4{FeCl(2,2′-bpy)}] (1), [Mo_3O_{12}{Fe(2,2′-bpy)}$_2$]·0.25 H_2O (2), and [Mo_4O_{15}{Fe(2,2′-bpy)}$_2$] (3)

	x	*y*	*z*	*U*(eq)		*x*	*y*	*z*	*U*(eq)
(1)									
Mo(1)	1891(1)	5307(1)	3394(1)	9(1)	C(2)	3379(7)	1998(2)	4222(4)	19(1)
Fe(2)	2977(1)	4184(1)	6197(1)	11(1)	C(3)	3735(7)	1481(2)	5253(4)	20(1)
Cl(1)	3361(2)	5403(1)	7014(1)	23(1)	C(4)	3811(7)	1741(2)	6524(4)	17(1)
O(1)	2300(5)	4444(1)	4334(2)	15(1)	C(5)	3451(6)	2504(2)	6718(4)	13(1)
O(2)	4078(4)	5888(2)	3657(3)	14(1)	C(6)	3409(6)	2828(2)	8033(4)	12(1)
O(3)	1236(5)	5062(2)	1768(3)	21(1)	C(7)	3441(6)	2392(3)	9146(4)	19(1)
O(4)	−82(4)	5867(2)	3782(3)	16(1)	C(8)	3467(7)	2748(3)	10330(4)	25(1)
N(1)	3117(5)	3005(2)	5708(3)	12(1)	C(9)	3462(7)	3532(3)	10390(5)	23(1)
N(2)	3358(5)	3600(2)	8075(3)	12(1)	C(10)	3386(6)	3940(2)	9235(4)	18(1)
C(1)	3106(6)	2753(2)	4486(4)	16(1)					
(2)									
Mo(1)	7981(1)	9315(1)	677(1)	16(1)	N(4)	7989(7)	13581(6)	833(5)	18(1)
Mo(2)	5475(1)	11664(1)	3429(1)	14(1)	C(1)	7797(9)	5677(9)	4639(7)	24(2)
Mo(3)	9372(1)	8539(1)	3345(1)	19(1)	C(2)	8126(9)	4340(8)	4970(7)	24(2)
Fe(1)	6235(1)	8431(1)	3584(1)	14(1)	C(3)	7524(10)	3645(9)	4631(8)	33(2)
Fe(2)	8781(1)	11526(1)	1440(1)	15(1)	C(4)	6582(9)	4339(8)	3991(7)	26(2)
O(1)	6868(8)	9276(6)	−18(6)	34(2)	C(5)	6279(8)	5691(8)	3692(7)	19(2)
O(2)	9669(7)	8499(6)	−62(5)	28(1)	C(6)	5226(8)	6491(8)	3066(7)	18(2)
O(3)	7630(6)	8385(5)	2068(4)	19(1)	C(7)	4451(9)	6000(8)	2708(7)	22(2)
O(4)	7740(6)	11007(5)	684(5)	19(1)	C(8)	3450(9)	6835(10)	2177(7)	27(2)
O(5)	7172(6)	11777(6)	2802(5)	21(1)	C(9)	3268(10)	8163(10)	1972(8)	29(2)
O(6)	5115(6)	11616(6)	4910(5)	21(1)	C(10)	4094(10)	8603(9)	2337(7)	25(2)
O(7)	4343(7)	13050(6)	2898(6)	31(2)	C(11)	10643(9)	11823(9)	2751(7)	25(2)
O(8)	5266(6)	10274(5)	3118(5)	20(1)	C(12)	11340(9)	12439(10)	3097(8)	31(2)
O(9)	7583(6)	8674(6)	4149(4)	19(1)	C(13)	11040(10)	13787(10)	2793(8)	33(2)
O(10)	10175(7)	8724(7)	4231(6)	34(2)	C(14)	10085(10)	14460(10)	2150(7)	29(2)
O(11)	10190(6)	6988(6)	3014(6)	30(1)	C(15)	9461(9)	13790(9)	1816(7)	22(2)
O(12)	9603(6)	9775(6)	2085(5)	23(1)	C(16)	8430(8)	14409(7)	1125(6)	17(2)
O(50)	12321(28)	9538(27)	4378(23)	34(6)	C(17)	7996(10)	15738(8)	773(7)	25(2)
N(1)	6890(6)	6345(6)	4017(5)	15(1)	C(18)	7074(10)	16229(9)	91(8)	29(2)
N(2)	5040(7)	7794(7)	2878(5)	17(1)	C(19)	6615(9)	15385(9)	−203(8)	28(2)
N(3)	9738(7)	12477(7)	2111(6)	19(1)	C(20)	7093(9)	14069(8)	181(7)	22(2)
(3)									
Mo(1)	−480(1)	9146(1)	1377(1)	12(1)	N(3)	−3615(5)	10816(5)	3798(4)	15(1)
Mo(2)	478(1)	11335(1)	3705(1)	12(1)	N(4)	−2409(5)	8169(5)	3972(4)	15(1)
Mo(3)	2009(1)	6990(1)	3674(1)	15(1)	C(1)	−1379(7)	13721(7)	1274(5)	24(1)
Mo(4)	3591(1)	7808(1)	1565(1)	19(1)	C(2)	−2162(7)	15081(7)	1393(5)	29(2)
Fe(1)	1251(1)	11116(1)	1061(1)	12(1)	C(3)	−1529(8)	15918(7)	1468(6)	31(2)
Fe(2)	−1511(1)	9578(1)	3903(1)	12(1)	C(4)	−129(7)	15391(6)	1418(5)	24(1)
O(1)	−342(4)	10663(4)	1027(3)	16(1)	C(5)	602(6)	14029(6)	1286(4)	14(1)
O(2)	1100(5)	7939(4)	1703(3)	23(1)	C(6)	2089(6)	13376(6)	1178(4)	17(1)
O(3)	−1127(5)	8556(4)	400(3)	18(1)	C(7)	2909(7)	14075(7)	1134(5)	24(1)
O(4)	−1573(4)	9422(4)	2415(3)	19(1)	C(8)	4290(7)	13366(7)	1011(5)	24(1)
O(5)	−1069(4)	11128(4)	3715(3)	17(1)	C(9)	4842(7)	11976(7)	947(5)	24(1)
O(6)	126(5)	12972(4)	3875(3)	23(1)	C(10)	3978(7)	11343(7)	1003(5)	22(1)
O(7)	1618(4)	10318(4)	4633(3)	14(1)	C(11)	−4137(6)	12163(6)	3706(4)	19(1)
O(8)	1314(4)	10857(4)	2535(3)	18(1)	C(12)	−5495(7)	12916(7)	3569(5)	25(1)
O(9)	341(4)	8263(4)	3952(3)	19(1)	C(13)	−6352(6)	12280(7)	3511(5)	27(2)
O(10)	1874(5)	5644(4)	3187(4)	26(1)	C(14)	−5824(6)	10901(7)	3611(5)	22(1)
O(11)	2846(5)	6454(5)	4759(3)	25(1)	C(15)	−4444(6)	10188(6)	3759(4)	17(1)
O(12)	3164(5)	7554(5)	2906(3)	24(1)	C(16)	−3773(6)	8700(6)	3895(4)	15(1)
O(13)	3895(6)	6441(5)	874(4)	34(1)	C(17)	−4470(6)	7893(7)	3942(5)	21(1)
O(14)	5127(5)	7869(6)	1686(4)	35(1)	C(18)	−3746(7)	6516(7)	4064(5)	26(2)
O(15)	2618(4)	9334(4)	885(3)	17(1)	C(19)	−2353(7)	5974(7)	4119(5)	26(1)
N(1)	−21(5)	13200(5)	1231(4)	15(1)	C(20)	−1718(6)	6838(6)	4077(5)	20(1)
N(2)	2627(5)	12030(5)	1100(4)	15(1)					

As illustrated in Figure 1c, [Mo_4O_{15}{Fe(2,2′-bpy)}$_2$] (**3**) exhibits a one-dimensional structure very similar to that observed for compound **2**. In the case of **3**, however, the adjacent iron centers are bridged by two {MoO_4} units and an {Mo_2O_7} unit, while **2** exhibits bridging through {MoO_4} tetrahedra, exclusively. Adjacent {Mo_2O_7} units in **3** alternate so as to occupy opposite sides of the chain as shown in Figure 2c. The length of the {Mo_2O_7} unit and the constraints thus imposed on the {FeN_2O_4} units that it bridges perturb the structure of the one-dimensional chains with respect to the chains of compound **2**.

Compounds **1**−**3** all share as a common motif a four-polyhedral ring which consists of two {MoO_4} tetrahedra and two {$FeXN_2O_3$} (X = Cl for **1**, O for **2** and **3**) octahedra. These polyhedra corner share such that each molybdenum center serves to bridge the two iron octahedra in the ring. Attachment to the next such four-ring is through the third corner sharing interaction of each molybdenum tetrahedron. As the additional {MoO_4} or {Mo_2O_7} linkages are incorporated in **2** and **3**, the basic four-ring remains intact as observed in Figure 1. However, the two iron centers in the four-polyhedra ring are now additionally linked through the aforementioned {MoO_4} or {Mo_2O_7} moieties. Thus, bridging of adjacent iron octahedra in **2** and **3** alternates between two molybdenum tetrahedra and either three molybdenum tetrahedra or two molybdenum tetrahedra and one dimolybdate bi-tetrahedral unit, respectively.

Table 3. Selected Bond Lengths (Å) and Angles (deg) for $[MoO_4\{FeCl(2,2'\text{-bpy})\}]$ (1), $[Mo_3O_{12}\{Fe(2,2'\text{-bpy})\}_2]\cdot 0.25\ H_2O$ (2), and $[Mo_4O_{15}\{Fe(2,2'\text{-bpy})\}_2]$ (3)

	bond length		angle		angle
		(**1**)			
Mo(1)−O(3)	1.707(3)	O(3)−Mo(1)−O(2)	109.14(14)	O(1)−Fe(2)−N(2)	164.29(12)
Mo(1)−O(2)	1.787(3)	O(3)−Mo(1)−O(4)	108.2(2)	O(4)[a]−Fe(2)−N(2)	83.93(13)
Mo(1)−O(4)	1.791(3)	O(2)−Mo(1)−O(4)	107.44(12)	O(2)[b]−Fe(2)−N(2)	88.83(13)
Mo(1)−O(1)	1.795(2)	O(3)−Mo(1)−O(1)	107.53(13)	N(1)−Fe(2)−N(2)	75.63(12)
Fe(2)−O(1)	1.944(3)	O(2)−Mo(1)−O(1)	112.03(13)	O(1)−Fe(2)−Cl(1)	97.50(8)
Fe(2)−O(4)[a]	1.992(3)	O(4)−Mo(1)−O(1)	112.37(14)	O(4)[a]−Fe(2)−Cl(1)	94.15(9)
Fe(2)−O(2)[b]	1.996(3)	O(1)−Fe(2)−O(4)[a]	89.95(13)	O(2)[b]−Fe(2)−Cl(1)	89.91(9)
Fe(2)−N(1)	2.144(3)	O(1)−Fe(2)−O(2)[b]	96.25(13)	N(1)−Fe(2)−Cl(1)	169.29(10)
Fe(2)−N(2)	2.170(3)	O(4)[a]−Fe(2)−O(2)[b]	172.10(11)	N(2)−Fe(2)−Cl(1)	97.37(9)
Fe(2)−Cl(1)	2.3030(11)	O(1)−Fe(2)−N(1)	90.33(11)	Mo(1)−O(1)−Fe(2)	135.8(2)
		O(4)[a]−Fe(2)−N(1)	93.16(12)	Mo(1)−O(2)−Fe(2)[b]	141.0(2)
		O(2)[b]−Fe(2)−N(1)	81.94(12)	Mo(1)−O(4)−Fe(2)[a]	141.4(2)
		(**2**)			
Mo(1)−O(1)	1.714(6)	O(1)−Mo(1)−O(2)	107.1(3)	O(9)−Fe(1)−N(2)	168.5(3)
Mo(1)−O(2)	1.778(6)	O(1)−Mo(1)−O(3)	108.1(3)	O(8)−Fe(1)−N(2)	91.1(2)
Mo(1)−O(3)	1.792(5)	O(2)−Mo(1)−O(3)	107.4(3)	O(6)[c]−Fe(1)−N(2)	91.4(2)
Mo(1)−O(4)	1.807(5)	O(1)−Mo(1)−O(4)	107.5(3)	O(3)−Fe(1)−N(2)	87.7(2)
Mo(2)−O(7)	1.721(6)	O(2)−Mo(1)−O(4)	113.0(3)	N(1)−Fe(1)−N(2)	75.8(3)
Mo(2)−O(6)	1.774(6)	O(3)−Mo(1)−O(4)	113.4(2)	O(12)−Fe(2)−O(2)[d]	93.7(3)
Mo(2)−O(5)	1.776(5)	O(7)−Mo(2)−O(6)	108.2(3)	O(12)−Fe(2)−O(4)	93.9(2)
Mo(2)−O(8)	1.792(5)	O(7)−Mo(2)−O(5)	108.5(3)	O(2)[d]−Fe(2)−O(4)	92.1(3)
Mo(3)−O(10)	1.706(7)	O(6)−Mo(2)−O(5)	108.0(3)	O(12)−Fe(2)−O(5)	92.3(2)
Mo(3)−O(11)	1.725(6)	O(7)−Mo(2)−O(8)	108.6(3)	O(2)[d]−Fe(2)−O(5)	173.3(2)
Mo(3)−O(12)	1.829(6)	O(6)−Mo(2)−O(8)	111.6(3)	O(4)−Fe(2)−O(5)	90.4(2)
Mo(3)−O(9)	1.836(5)	O(5)−Mo(2)−O(8)	111.8(3)	O(12)−Fe(2)−N(4)	172.3(3)
Fe(1)−O(9)	1.932(6)	O(10)−Mo(3)−O(11)	106.7(3)	O(2)[d]−Fe(2)−N(4)	86.5(2)
Fe(1)−O(8)	1.971(6)	O(10)−Mo(3)−O(12)	106.4(3)	O(4)−Fe(2)−N(4)	93.7(2)
Fe(1)−O(6)[c]	1.987(5)	O(11)−Mo(3)−O(12)	111.1(3)	O(5)−Fe(2)−N(4)	87.2(2)
Fe(1)−O(3)	2.015(5)	O(10)−Mo(3)−O(9)	106.8(3)	O(12)−Fe(2)−N(3)	97.3(3)
Fe(1)−N(1)	2.146(7)	O(11)−Mo(3)−O(9)	109.7(3)	O(2)[d]−Fe(2)−N(3)	86.9(3)
Fe(1)−N(2)	2.159(7)	O(12)−Mo(3)−O(9)	115.6(3)	O(4)−Fe(2)−N(3)	168.7(2)
Fe(2)−O(12)	1.912(6)	O(9)−Fe(1)−O(8)	99.1(2)	O(5)−Fe(2)−N(3)	89.4(2)
Fe(2)−O(2)[d]	1.981(6)	O(9)−Fe(1)−O(6)[c]	93.8(2)	N(4)−Fe(2)−N(3)	75.0(3)
Fe(2)−O(4)	1.982(6)	O(8)−Fe(1)−O(6)[c]	91.5(2)	Mo(1)−O(2)−Fe(2)[d]	148.8(4)
Fe(2)−O(5)	2.003(5)	O(9)−Fe(1)−O(3)	86.7(2)	Mo(1)−O(3)−Fe(1)	142.2(3)
Fe(2)−N(4)	2.161(7)	O(8)−Fe(1)−O(3)	91.0(2)	Mo(1)−O(4)−Fe(2)	121.8(3)
Fe(2)−N(3)	2.168(7)	O(6)[c]−Fe(1)−O(3)	177.3(2)	Mo(2)−O(5)−Fe(2)	145.4(3)
		O(9)−Fe(1)−N(1)	94.4(2)	Mo(2)−O(6)−Fe(1)[c]	148.0(4)
		O(8)−Fe(1)−N(1)	166.4(2)	Mo(2)−O(8)−Fe(1)	126.3(3)
		O(6)[c]−Fe(1)−N(1)	85.2(2)	Mo(3)−O(9)−Fe(1)	124.4(3)
		O(3)−Fe(1)−N(1)	92.1(2)	Mo(3)−O(12)−Fe(2)	143.1(3)
		(**3**)			
Mo(1)−O(2)	1.741(4)	O(2)−Mo(1)−O(4)	108.2(2)	O(1)−Fe(1)−N(2)	167.7(2)
Mo(1)−O(4)	1.770(4)	O(2)−Mo(1)−O(3)	109.6(2)	O(8)−Fe(1)−N(2)	91.2(2)
Mo(1)−O(3)	1.777(4)	O(4)−Mo(1)−O(3)	108.6(2)	O(15)−Fe(1)−N(1)	171.1(2)
Mo(1)−O(1)	1.788(4)	O(2)−Mo(1)−O(1)	109.4(2)	O(3)[e]−Fe(1)−N(1)	87.9(2)
Mo(2)−O(6)	1.701(4)	O(4)−Mo(1)−O(1)	109.7(2)	O(1)−Fe(1)−N(1)	91.8(2)
Mo(2)−O(8)	1.788(4)	O(3)−Mo(1)−O(1)	111.3(2)	O(8)−Fe(1)−N(1)	90.0(2)
Mo(2)−O(7)	1.795(4)	O(6)−Mo(2)−O(8)	108.4(2)	N(2)−Fe(1)−N(1)	76.0(2)
Mo(2)−O(5)	1.798(4)	O(6)−Mo(2)−O(7)	109.9(2)	O(9)−Fe(2)−O(5)	95.5(2)
Mo(3)−O(10)	1.704(5)	O(8)−Mo(2)−O(7)	107.4(2)	O(9)−Fe(2)−O(7)[f]	91.2(2)
Mo(3)−O(11)	1.709(5)	O(6)−Mo(2)−O(5)	109.2(2)	O(5)−Fe(2)−O(7)[f]	94.4(2)
Mo(3)−O(9)	1.814(4)	O(8)−Mo(2)−O(5)	109.6(2)	O(9)−Fe(2)−O(4)	92.2(2)
Mo(3)−O(12)	1.900(4)	O(7)−Mo(2)−O(5)	112.3(2)	O(5)−Fe(2)−O(4)	90.3(2)
Mo(4)−O(13)	1.705(5)	O(10)−Mo(3)−O(11)	106.7(2)	O(7)[f]−Fe(2)−O(4)	173.9(2)
Mo(4)−O(14)	1.720(5)	O(10)−Mo(3)−O(9)	109.5(2)	O(9)−Fe(2)−N(3)	172.5(2)
Mo(4)−O(15)	1.809(4)	O(11)−Mo(3)−O(9)	108.1(2)	O(5)−Fe(2)−N(3)	91.5(2)
Mo(4)−O(12)	1.906(4)	O(10)−Mo(3)−O(12)	112.3(2)	O(7)[f]−Fe(2)−N(3)	91.0(2)
Fe(1)−O(15)	1.924(4)	O(11)−Mo(3)−O(12)	103.3(2)	O(4)−Fe(2)−N(3)	85.1(2)
Fe(1)−O(3)[e]	2.001(4)	O(9)−Mo(3)−O(12)	116.3(2)	O(9)−Fe(2)−N(4)	96.2(2)
Fe(1)−O(1)	2.004(4)	O(13)−Mo(4)−O(14)	105.7(3)	O(5)−Fe(2)−N(4)	167.5(2)
Fe(1)−O(8)	2.008(4)	O(13)−Mo(4)−O(15)	111.0(2)	O(7)[f]−Fe(2)−N(4)	89.9(2)
Fe(1)−N(2)	2.133(5)	O(14)−Mo(4)−O(15)	103.2(2)	O(4)−Fe(2)−N(4)	84.8(2)
Fe(1)−N(1)	2.146(5)	O(13)−Mo(4)−O(12)	112.2(2)	N(3)−Fe(2)−N(4)	76.7(2)
Fe(2)−O(9)	1.936(4)	O(14)−Mo(4)−O(12)	101.1(2)	Mo(1)−O(1)−Fe(1)	129.8(2)
Fe(2)−O(5)	1.968(4)	O(15)−Mo(4)−O(12)	121.4(2)	Mo(1)−O(3)−Fe(1)[e]	134.2(2)
Fe(2)−O(7)[f]	1.989(4)	O(15)−Fe(1)−O(3)[e]	91.0(2)	Mo(1)−O(4)−Fe(2)	138.5(2)
Fe(2)−O(4)	2.035(4)	O(15)−Fe(1)−O(1)	97.1(2)	Mo(2)−O(5)−Fe(2)	133.8(2)
Fe(2)−N(3)	2.132(5)	O(3)[e]−Fe(1)−O(1)	89.5(2)	Mo(2)−O(7)−Fe(2)[f]	130.9(2)
Fe(2)−N(4)	2.154(5)	O(15)−Fe(1)−O(8)	91.3(2)	Mo(2)−O(8)−Fe(1)	148.2(2)
		O(3)[e]−Fe(1)−O(8)	177.8(2)	Mo(3)−O(9)−Fe(2)	165.6(3)
		O(1)−Fe(1)−O(8)	89.9(2)	Mo(3)−O(12)−Mo(4)	140.8(3)
		O(15)−Fe(1)−N(2)	95.2(2)	Mo(4)−O(15)−Fe(1)	141.8(2)
		O(3)[e]−Fe(1)−N(2)	88.8(2)		

[a] $-x, -y+1, -z+1$ (symmetry transformations used to generate equivalent atoms). [b] $-x+1, -y+1, -z+1$. [c] $-x+1, -y+2, -z+1$. [d] $-x+2, -y+2, -z$. [e] $-x, -y+2, -z$. [f] $-x, -y+2, -z+1$.

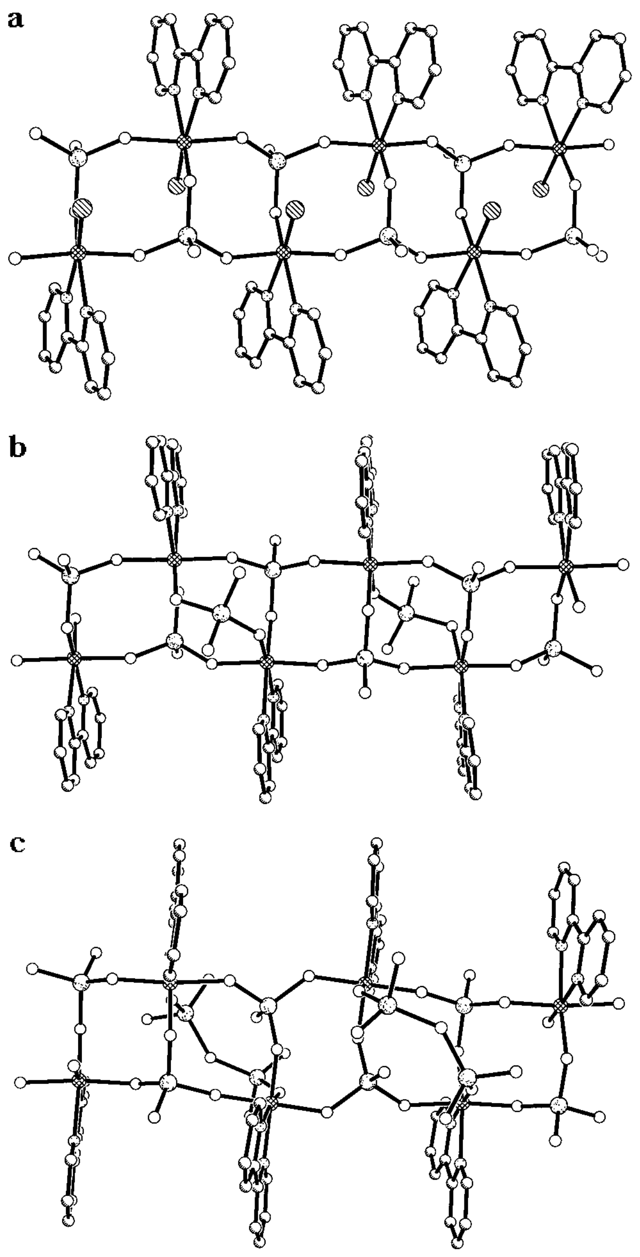

Figure 1. Views of the one-dimensional chains of (a) [$MoO_4\{FeCl(2,2'\text{-bpy})\}$] (**1**), (b) [$Mo_3O_{12}\{Fe(2,2'\text{-bpy})\}_2$]·0.25 H_2O (**2**), and (c) [$Mo_4O_{15}\{Fe(2,2'\text{-bpy})\}_2$] (**3**). Iron atoms are denoted by crosshatched circles, molybdenums by stippled circles, chloride atoms by circles with lines from top left to bottom right, and oxygens by open circles.

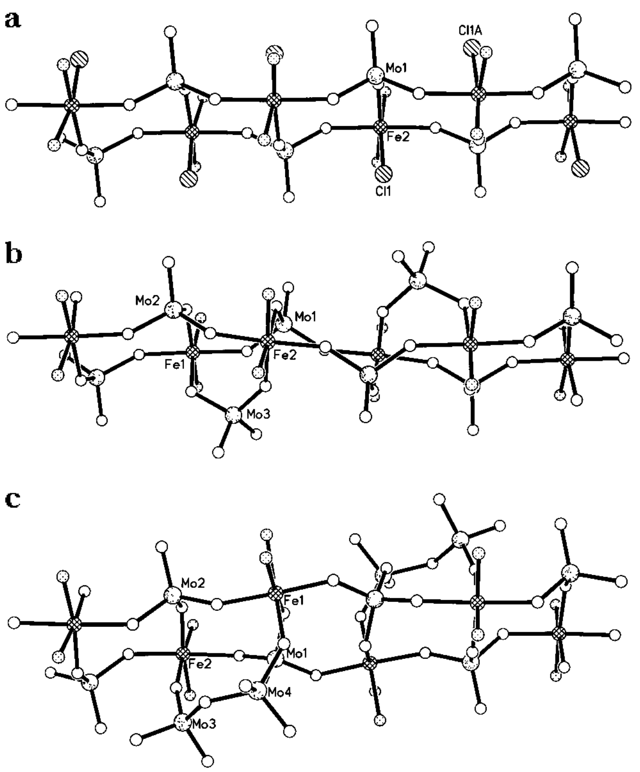

Figure 2. A view of the chains of (a) [$MoO_4\{FeCl(2,2'\text{-bpy})\}$] (**1**), (b) [$Mo_3O_{12}\{Fe(2,2'\text{-bpy})\}_2$]·0.25 H_2O (**2**), and (c) [$Mo_4O_{15}\{Fe(2,2'\text{-bpy})\}_2$] (**3**), emphasizing the relative orientation of the chlorides in **1** and the {MoO_4} and {Mo_2O_7} substituents in **2** and **3**, respectively. Atom types as for Figure 1.

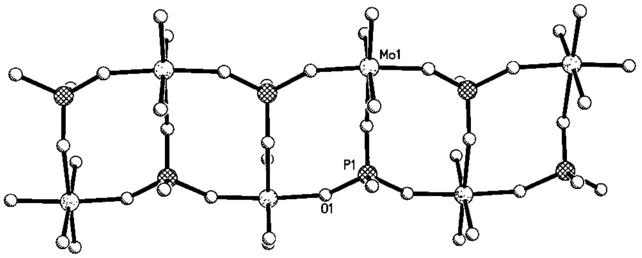

Figure 3. A view of the chain of $Mo(OH)_3PO_4$. Molybdenum atoms are denoted by stippled circles, phosphorus by cross-hatched circles and oxygens by open circles.

It should be noted that the repeating four-polyhedra rings observed in **1**–**3** bear a striking resemblance to the chains observed in $Mo(OH)_3PO_4$, shown in Figure 3.[29] In the latter structure, the chains contain alternating {MoO_6} octahedra and {PO_4} tetrahedra, whereas the compounds reported herein contain iron octahedra and molybdenum tetrahedra.

Comparison of the one-dimensional chains of **1**–**3** in Figure 2 illustrates the marked changes in the chain structures as additional linkers are added between adjacent iron sites. The fundamental motif present in all three compounds is the unit of two bridging {$MoO_{3/2}O$} tetrahedra between adjacent iron octahedra. When the terminal chlorides on adjacent iron centers in the basic chain of compound **1** are replaced by {$MoO_{2/2}O_2$} or {Mo_2O_7} bridges, seen in Figure 2, the chain becomes increasingly distorted. The repeat distance of the ribbon in the three compounds varies from 13.72 (6.86 × 2) Å in **1** to 13.69 Å in **2** while **3** has a repeat distance of 13.56 Å. This variation of the repeat distance is due to the aforementioned distortion of the chain.

Examination of the relative orientations of adjacent symmetry-related chains of **1**–**3** reveals that although these compounds are similar in their chain construction, the packing varies greatly and is dependent upon the orientation of the 2,2′-bipyridine rings along the chains. Compound **1**, shown in Figure 4a, packs such that each 2,2′-bipyridine ring interacts with rings from two adjacent chains. The closest contact between adjacent rings in **1** is 3.094 Å. Examination of the structure of **1** reveals that the bipyridine rings interact in such a way that sinusoidal virtual "layers" of bipyridine appear to alternate with areas containing the inorganic portion of **1**.

---

[29] Kierkegaard, P. *Acta Chem. Scand.* **1958**, *12*, 1701.

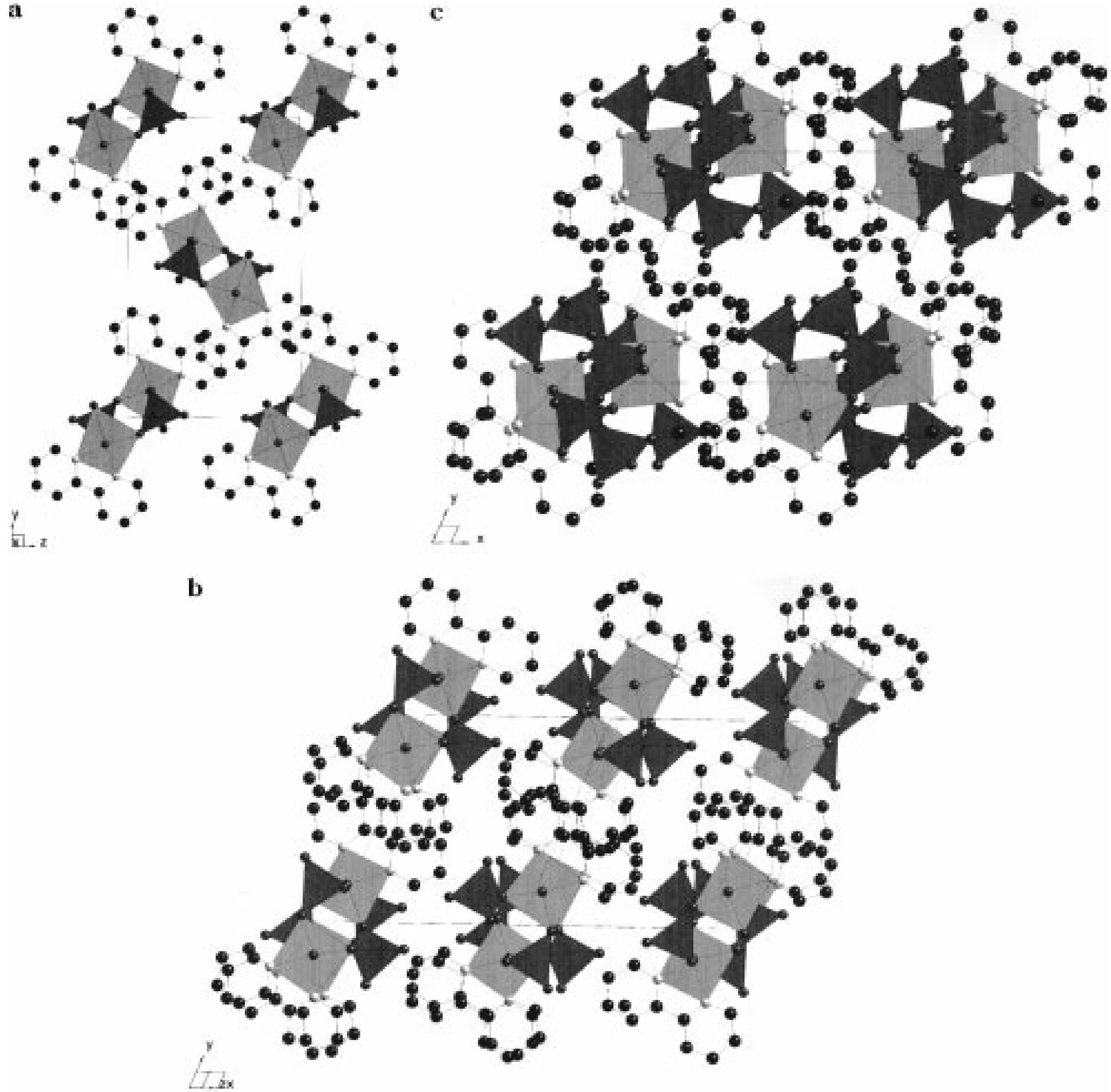

Figure 4. Views of the unit cell packing of adjacent symmetry-related chains with unit cells outlined in (a) [MoO_4{FeCl(2,2′-bpy)}] (**1**), (b) [Mo_3O_{12}{Fe(2,2′-bpy)}$_2$]·0.25 H_2O (**2**), and (c) [Mo_4O_{15}{Fe(2,2′-bpy)}$_2$ (**3**). (In all cases the Fe octahedra and Mo tetrahedra have been shown as polyhedra while the ball-and-stick motif has been used to show the positions of the bipyridine rings.)

The chains of **2** exhibit some modifications due to the addition of the {MoO_4} linker between adjacent iron centers. This perturbation is evidenced by the slight irregularity in the alignment of adjacent bipyridine rings on the chain with respect to one another. Examination of the packing of **2**, in Figure 4b, shows that each bipyridine on the chain stacks with bipyridines on one adjacent chain, with the closest contact between rings being 3.277 Å. As noted previously, compound **3** exhibits significant modification of the one-dimensional chain due to the addition of the {Mo_2O_7} linker, leading to even greater irregularity in the alignment of adjacent bipyridine substituents on the chain. Consequently, the bipyridine rings alternate side-to-side on the chain, hindering effective overlap with adjacent chains. Examination of the packing of **3**, shown in Figure 4c, shows parallel chains located such that their bipyridine rings interdigitate with the closest interactions greater than 3.4 Å.

While bearing some superficial resemblance to the previously reported one-dimensional [Ni(2,2′-bpy)$_2$$Mo_4O_{13}$] (**A**) and [Cu(2,2′-bpy)Mo_2O_7] (**B**) and the two-dimensional [Co(2,2′-bpy)Mo_3O_{10}] (**C**),[15] compounds **1**−**3** exhibit unique structural features. While materials **A**−**C** are constructed from either molybdenum clusters or chains, compounds **1**−**3** are exclusively constructed from discrete {MoO_4}$^{2-}$ or {MoO_4}$^{2-}$ and {Mo_2O_7}$^{2-}$ units, linked through {Fe(2,2′-bpy)}$^{2+}$ moieties. While one-dimensional chains are formed in **1**−**3**, these are not one-dimensional molybdenum oxide chains with {Mo−

O−Mo} linkages and peripheral metal/organic components but, in contrast, are polymers in which the metal/organic unit is an integral part of the one-dimensional structure.

Conclusions

The isolation and characterization of compounds **1**−**3** reinforce the observation that small amounts of organic material may profoundly influence the structures of metal oxide phases. It is evident that the combination of hydrothermal techniques and incorporation of organic components affords a powerful method for the modification of metal oxide structures and for the isolation of new metal oxide compositions. While it is premature to refer to such chemistry as “crystal engineering,” judicious choice of organic constituents allows for passivation of metal oxide coordination spheres leading to low-dimensional materials, variable tethering of oxide sites, sculpting of cavities, and preparation of unexpected mixed-metal/oxide/ligand composites. While predictability is yet lacking, structural and compositional diversity are not.

We are currently studying the thermal treatment of **1**−**3** and related mixed-metal/oxide/ligand composites as starting materials for new mixed-metal oxides. In most cases, the organic constituent may be removed at fairly low temperatures to afford mixed-metal oxides whose structures and identities are under investigation.

Acknowledgment. The work at Syracuse University was supported by NSF Grant CHE9617232. The authors also thank Dr. Robert A. Sparks and Bruker Analytical X-ray Systems, Inc. (formerly Siemens Analytical Instruments, Inc.) for allowing the use of their beta test version of the Non-merohedral Twinning Software.

Supporting Information Available: Tables of experimental details, atomic coordinates, and temperature factors, anisotropic temperature factors, bond lengths and angles, and calculated hydrogen atom positions for compounds **1**−**3** (17 pages). Ordering information given on any current masthead page.

CM9707667